J Solid State Electrochem (2008) 12:655–661
DOI 10.1007/s10008-007-0395-0

ORIGINAL PAPER

Electrocatalytic activity of hemoglobin in sodium alginate/SiO_2 nanoparticle/ionic liquid $BMIMPF_6$ composite film

Wei Sun · Dandan Wang · Jianghua Zhong · Kui Jiao

Received: 22 April 2007 / Revised: 8 July 2007 / Accepted: 13 July 2007 / Published online: 2 October 2007

Abstract A novel biocompatible composite film containing sodium alginate (SA), room temperature ionic liquid 1-butyl-3-methylimidazolium hexafluorophosphate ($BMIMPF_6$), SiO_2 nanoparticle, and hemoglobin (Hb) was fabricated and covered on the surface of a traditional carbon paste elecrode (CPE). The immobilized Hb on the electrode surface showed good direct electrochemical behaviors, and a pair of quasi-reversible redox peaks of Hb was obtained, which indicated that the direct electron transfer of Hb with the electrode surface had been achieved. The SA/nano-SiO_2/$BMIMPF_6$/Hb/CPE showed dramatically electrocatalytic activity to the reduction of trichloroacetic acid, hydrogen peroxide (H_2O_2), and oxygen (O_2). The kinetic parameters for the electrocatalytic reactions were evaluated. The composite film showed the potential to the biosensor and biocatalysis.

Keywords Hemoglobin · Electrochemistry · Carbon paste electrode · Electrocatalysis · Direct electron transfer · 1-butyl-3-methylimidazolium hexafluorophosphate · SiO_2 nanoparticle

Introduction

Direct electrochemistry of redox protein on the electrode has attracted great interests in recent years for its potential applications in the fields of biosensors and bioreactors. As the electrochemical behaviors of protein or enzyme on the bare working electrode cannot be achieved due to the difficulty of the direct electron transfer and denaturation of adsorbed protein. Most of the reports are focused on the film-modified electrode for protein, which was named as protein film electrochemistry. Different kinds of modifiers such as surfactant [1, 2], hydrogel [3, 4], biopolymer [5, 6], inorganic [7, 8] or organic composite matrix [9, 10], and nanoparticles [11, 12] had been used to promote the direct electron transfer efficiency and retain the native conformation of protein. Some of the protein films showed good electrocatalytic activities to various substrates.

Recently, the application of room temperature ionic liquids (RTILs) in the protein electrochemistry had aroused great interests. RTILs are ionic compounds consisting of organic cations and various anions, which are in liquid state at ambient temperature and belong to non-aqueous polar solvents. They have many unique physicochemical characteristics such as relatively high ionic conductivity, high chemical and thermal stability, negligible vapor pressure, and wide electrochemical windows [13–15]. RTILs can be used to dissolve and extract many organic or ion substances. Proteins such as enzyme can also keep their activity and stability in the RTILs better than in the conventional organic solvent or aqueous solution. Due to the higher ionic conductivity and wider electrochemical windows, RTILs have the potentials in the field of electrochemistry and electroanalysis. Compton and Laszlo [16] and Endres [17] had listed the recent developments of RTILs in the electrochemistry. RTILs can be used not only as supporting electrolyte but also as the modifier in the electrochemical studies. Opallo et al. had investigated the ion transfer process occurring across RTILs/aqueous solution interface using dif-

W. Sun (✉) · D. Wang · J. Zhong · K. Jiao
College of Chemistry and Molecular Engineering,
Qingdao University of Science and Technology,
Qingdao, Shandong 266042, China
e-mail: sunwei@qust.edu.cn

ferent materials such as basal plane pyrolytic graphite [18], glassy carbon [19], carbon ionic liquid electrode (CILE) [20] as the electrode supports for RTILs phase. Li et al. entrapped horseradish peroxidase or hemoglobin (Hb) into a chitosan-$BMIMBF_4$ composite materials to fabricated a mediator-free biosensor [21, 22]. Zhang et al. [23] investigated the electrochemical functionalization single-walled carbon nanotubes (CNT) in large quantities at a RTILs-supported three-dimensional network electrode. Dong et al. fabricated a microperoxidase-11(MP-11)/carbon nanomaterials/RTILs composite film, which could be used to achieve the efficient electron transfer between the electrode and the protein [24]. Sun et al. [25] also investigated the direct electrochemistry of Hb in the sodium alginate (SA) film on a $BMIMPF_6$-modified carbon paste electrode. Other kinds of protein/RTILs composite materials with clay [26], CNT [27], sol–gel [28] etc. had also been reported. RTILs can also be used as a new kind of binder in carbon-paste-modified electrode. Maleki et al. [29] applied *N*-octylpyridinum hexafluorophosphate as binder for the construction of a high-performance carbon composite electrode and carefully investigated the electrochemical behaviors of CILE to different kinds of organic and inorganic electroactive compounds. Sun also combined *N*-butylpyridinium hexafluorophosphate ($BPPF_6$) with carbon powder to make a $BPPF_6$-modified carbon paste electrode [30]. Some organic substances such as uric acid [31], dopamine [32], nitric oxide [33], and ascorbic acid [34] had been successfully detected on the RTILs modified electrode by electrochemical method.

In this paper, Hb was mixed homogeneously with SA and $BMIMPF_6$, SiO_2 nanoparticles to form a novel bionanocomposite matrix and further modified on the surface of a traditional carbon paste electrode (CPE) to form a mediator-free biosensor. SA is a linear hydrophilic polysaccharide composed of β-D-mannuronic (M) and α-L-guluronic (G) acids. It is biocompatible, biodegradable, nontoxic natural biopolymer, and can be used as films for Hb immobilization. SiO_2 nanoparticles have the advantages such as good biocompatibility, large surface area, plentiful surface charges, and good dispersing property in water. $BMIMPF_6$ decomposes at a temperature of more than 200 °C and is a benign solvent with higher hydrophobicity and weaker hydrogen bond ability. By mixing SA, nano-SiO_2, $BMIMPF_6$ and Hb together, a homogeneous gel was formed. After it was applied on the electrode surface and a stable film was formed at room temperature, Hb can retain its bioactivity in the film, and the direct electron transfer with the electrode was achieved, which was attributed to biocompatibility microenvironments of SA and nano-SiO_2 and the inherent ionic conductivity of $BMIMPF_6$. The SA/nano-SiO_2/$BMIMPF_6$/Hb/CPE showed good electrocatalytic activity to the reduction of trichloroacetic acid (TCA), hydrogen peroxide (H_2O_2) and oxygen (O_2).

Experimental

Reagents

Bovine hemoglobin (Hb, MW 64500) was purchased from Tianjin Chuanye Biochemical. Room temperature ionic liquid 1-butyl-3-methylimidazolium hexafluorophosphate ($BMIMPF_6$) was from Hangzhou Kemer Chemical. SA was obtained from Tianjin Yuanhang Chemical. Twenty nanometers nano-SiO_2 was kindly provided by Department of Material Chemistry of our university, which was prepared according to the methods of Luo et al. [35]. Other chemicals such as TCA, hydrogen peroxide (H_2O_2) were of analytical reagents grade and used without further purification. Phosphate buffer solutions (PBS; 0.1 mol/l) with various pH values were prepared by mixing stock standard solutions of K_2HPO_4 and KH_2PO_4 and were adjusted the pH with 0.1 mol/l H_3PO_4 or NaOH. All aqueous solutions were made up with twice-distilled water.

Apparatus

Cyclic voltammetric measurements were performed on a CHI 840B electrochemical analyzer, and electrochemical impedance spectroscopy was performed on a CHI 750B electrochemical analyzer (Shanghai CH Instrumentation, China). The electrochemical cell was assembled with a conventional three-electrode system: a Hb-bionanocomposite-hybrid-film-modified carbon paste working electrode (CPE), a platinum wire auxiliary electrode, a saturated calomel reference electrode (SCE). All the solutions were deaerated by highly pure nitrogen for 30 min and kept at nitrogen atmosphere during the experiments.

Electrode preparation

The CPE was prepared by thoroughly mixing of graphite powder with paraffin at a ratio of 70:30 (*w*/*w*) in an agate mortar. The homogeneous paste was packed into a cavity of glass tube with the diameter of 4.2 mm. The electrical contact was obtained with a copper wire connected to the paste in the end of tube. The surface of CPE was smoothed with a weighing paper just before use.

The Hb-modified CPE was prepared according to the following procedure. Forty microliters of $BMIMPF_6$ and 0.8 mg of nano-SiO_2 were ground in an agate mortar for 30 min to form the gel phase. Then, a mixture solution of 50 μl SA hydrogel (4 mg/ml) and 5 mg Hb were added and further ground for 20 min. Finally, 5 μl the mixture was pipetted on the freshly polished surface of the CPE, and then the electrode was placed to stable for more than 1 h. A 10-ml beaker was covered over the surface of electrode so that a more uniform film could be formed on the electrode surface.

Results and discussion

Direct electrochemistry

Figure 1 showed the cyclic voltammograms of different modified CPE in 0.1 M pH 7.0 PBS at the scan rate of 100 mV/s. Due to the partly dissolving of the ionic liquids and the different compositions of the bionanocomposite film, the voltammetric responses of the SA/nano-SiO_2/$BMIMPF_6$/Hb film electrodes were unstable in the solution at the beginning. However, after cyclic sweeps for 15 cycles, the electrochemical signals turned to be stable. So, all the cyclic voltammograms of SA/nano-SiO_2/$BMIMPF_6$/Hb/CPE were recorded after 15 cyclic sweeps. It can be seen that a pair of quasi-reversible redox peaks appeared on SA/nano-SiO_2/$BMIMPF_6$/Hb-modified CPE (curve e), while no redox peaks appeared at other modified CPE (curve a, b, c), which indicated that the peaks were attributed to the direct electron transfer of Hb in the film on the electrode. There was a pair of very small redox peaks on the SA–$BMIMPF_6$–Hb/CPE (curve d), which indicated that the presence of SiO_2 nanoparticles can greatly enhance the direct electron transfer. From curve e, the anodic and cathodic peak appeared at −0.185 and −0.335 V (vs SCE), respectively. The formal potential ($E^{0\prime}$), which is calculated as the midpoint of the redox peak potential, was −0.26 V (vs SCE), and the peak-to-peak separation (ΔE_p) at the scan rate of 100 mV/s was calculated as 150 mV.

Figure 2 demonstrated the cyclic voltammograms of the SA/nano-SiO_2/$BMIMPF_6$/Hb/CPE at various scan rates in 0.1 mol/l pH 7.0 PBS. It can be seen that the peak currents increased along with the increase of the scan rate, which indicated that all the electroactive ferric Hb is reduced to ferrous Hb on the forward scan and the ferrous Hb produced is reoxidized to ferric Hb on the reverse scan. The plot of peak current vs scan rate was linear from 100 to 500 mV/s. All these results indicated that the redox reaction was an adsorption-controlled electron transfer process.

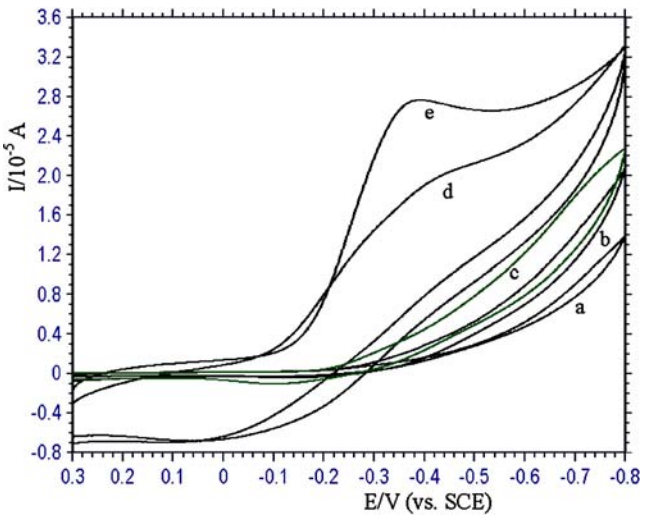

Fig. 1 Cyclic voltammograms of **a** CPE, **b** nano-SiO_2/$BMIMPF_6$/CPE, **c** SA/nano-SiO_2/$BMIMPF_6$/CPE, **d** SA/$BMIMPF_6$/Hb/CPE, and **e** SA/nano-SiO_2/$BMIMPF_6$/Hb/CPE in 0.1 mol/l pH 7.0 PBS with the scan rate as 100 mV/s

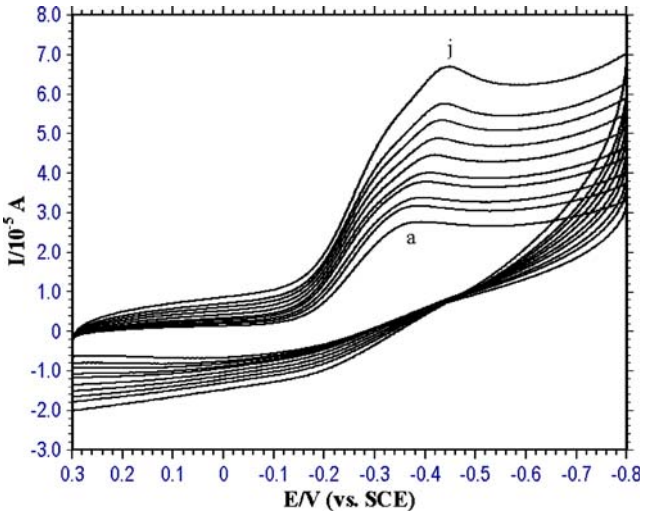

Fig. 2 Cyclic voltammograms of the SA/nano-SiO_2/$BMIMPF_6$/Hb/CPE in 0.1 mol/l pH 7.0 PBS with different scan rates (from *a* to *j*, 100, 150, 200, 250, 300, 350, 400, 450 and 500 mV/s)

As seen from Fig. 2, the peak-to-peak separation was also increased with the scan rate. By integrating the cyclic voltammetric peak at the scan rate from 100 to 500 mV/s, the total amount of charge (Q) passed through the electrode for the reduction or the oxidation reaction of Hb on the film can be obtained, and the value of Q was independent of the scan rate. For an adsorption electrochemical process, the surface concentration (Γ*) of electroactive substance can be calculated with the following equation: $Q=n\,F\,A\,\Gamma^*$, where n is the number of electron transferred, F is Faraday's constant, A is the geometric area of electrode. According to this method, the average surface concentration of electroactive Hb (Γ^*) was estimated as 8.64×10^{-10} mol/cm^2 assuming one electron transfer reaction. The value obtained was about 45.7 times higher than that of the theoretical monolayer about 1.89×10^{-11} mol/cm^2 [36]. The result indicated that several layers of Hb entrapped in the bionanocomposite film participated in the electron-transfer process. The relative amount of electroactive Hb on the electrode surface was 2.78% of the total amount of Hb deposited on the electrode surface, which was higher than that in Lu et al. [21]. The results demonstrated that the composite film can greatly retain the activity of Hb. The thickness of the film, which was calculated by the amount of the gel and the surface area of electrode, was about 0.36 mm.

The effect of buffer pH on the formal potential of Hb immobilized in the film was also investigated. With the

increase of buffer pH value from 4.0 to 9.0, both the reduction and oxidation peak potentials showed no significant changes. As the ionic liquids $BMIMPF_6$ was hydrophobic, the changes of pH value of external solution have no influences on the Hb molecules in the inner film, so the formal potential showed no changes with different pH of buffer solution.

After electrooxidation of Hb local deficiency of charge within RIIL phase occurred, the reaction has to be followed by ion transfer across IL/H_2O interface [18]. The equation is followed by cation K^+ injection into ionic liquid:

$$\text{Hb (III)} + e + K^+_{(aq)} \rightarrow \text{Hb Fe(II)} + K^+_{(film)}$$

can lower the overpotential of the reduction of TCA for at least 0.8 V with the increase of the reduction peak current of Hb Fe(III). The catalytic efficiency (I_c/I_d) of Hb Fe(III) was decreased with the increase of scan rate, which also was the characteristic of electrocatalytic reduction of TCA [37]. And the catalytic reduction equation for TCA can be expressed as follows:

$$\text{Hb Fe(III)} + e + K^+_{(aq)} \rightarrow \text{Hb Fe(II)} + K^+_{(film)}$$

$$Cl_3CCOOH \leftrightarrow Cl_3CCOO^- + H^+ \quad pK_a = 0.89$$

$$2\ \text{Hb Fe(II)} + K^+_{(film)} + Cl_3CCOO^-_{(aq)} + H_2O \rightarrow 2\,\text{Hb Fe(III)} + K^+_{(aq)} + Cl_2CHCOO^-_{(aq)} + Cl^-_{(aq)} + OH^-_{(aq)}$$

Electrocatalytic behaviors

The SA/nano-SiO_2/$BMIMPF_6$/Hb/CPE showed good electrocatalytic activity to various substances such as TCA, hydrogen peroxide (H_2O_2), and oxygen (O_2). The catalytic behaviors were recorded by cyclic voltammetry.

The SA/nano-SiO_2/$BMIMPF_6$/Hb/CPE showed good electrocatalytic reduction to TCA, and the results were shown in Fig. 3. At the bare CPE, the direct electrochemical reduction of TCA appeared at the potential of −1.0 V (vs SCE; curve b). While on the Hb-modified electrode, after the addition of TCA into a pH 7.0 PBS, an obvious increase of the reduction peak of Hb Fe(III) was observed at −0.214 V, with the Hb Fe(II) oxidation peak current decreased. The more TCA added, the higher the reduction peak current appeared (curve c–g). Therefore, the Hb-modified electrode

As shown in Fig. 3, the reduction peak currents increased with the increase of the TCA concentration in solution. A linear relationship was obtained between the reduction peak current and the TCA concentration in the range from 12.0 to 46.0 mmol/l with the linear regression equation as i_{pc} (μA)= 0.38 C (mmol/l)+9.24 (n=7, γ=0.997). Ten independent determinations at a TCA concentration of 40.0 mmol/l showed a relative standard deviation of 4.6%, which displayed good reproducibility of the measurements.

The electrocatalytic reduction to H_2O_2 was also carefully investigated, and the cyclic voltammograms were shown in Fig. 4. When different amounts of H_2O_2 were added into pH 7.0 PBS, an obvious increase of reduction peak current at −0.39 V was observed with a complete disappearance of the oxidation peak current (curve c–f), which indicated that the Hb immobilized in the film showed excellent electro-

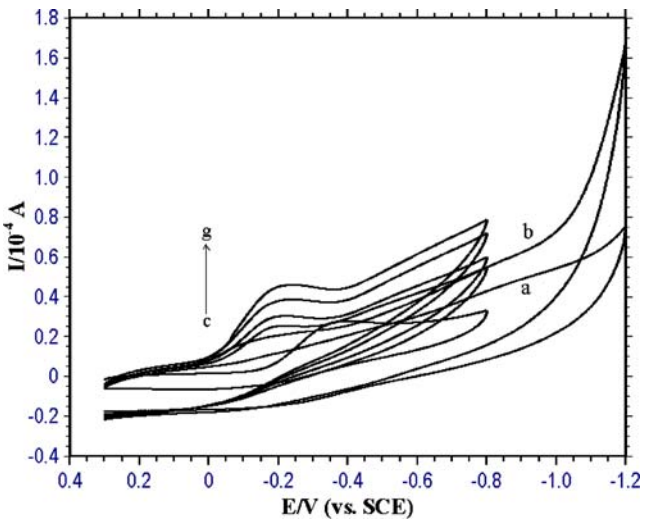

Fig. 3 Cyclic voltammograms of SA/nano-SiO_2/$BMIMPF_6$/CPE in 0.1 mol/l pH 7.0 PBS containing **a** 0 and **b** 12.0 mmol/l TCA solution, and SA/nano-SiO_2/$BMIMPF_6$/Hb/CPE in 0.1 mol/l pH 7.0 PBS containing 0, 12.0, 24.0, 36.0, 46.0 mmol/l TCA (curve *c–g*), respectively, with the scan rate as 100 mV/s

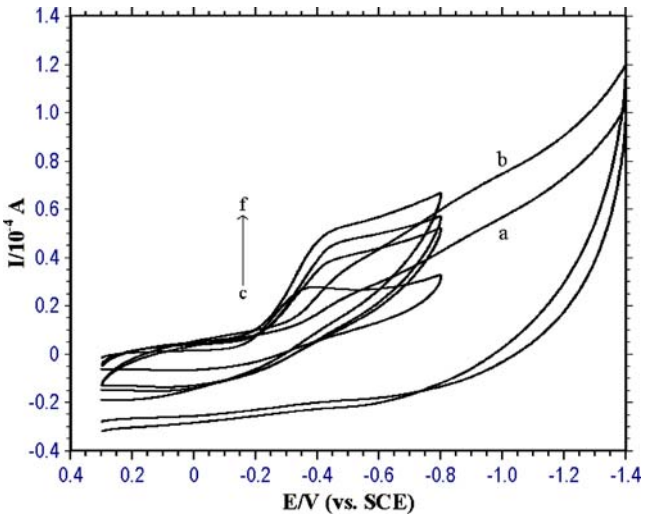

Fig. 4 Cyclic voltammograms of SA/nano-SiO_2/$BMIMPF_6$/CPE in 0.1 mol/l pH 7.0 PBS containing **a** 0 and **b** 2.0 μmol/l H_2O_2 solution, and SA/nano-SiO_2/$BMIMPF_6$/Hb/CPE in 0.1 mol/l pH 7.0 PBS buffer solution containing 0, 2.0, 4.0, 10.0 μmol/l H_2O_2 solution (curve *c–f*), respectively, with the scan rate as 100 mV/s

catalytic activity towards the reduction of H_2O_2. The reduction peak current was increased and proportional to the H_2O_2 concentration in the range of 2.0~10.0 μmol/l. When the concentration of H_2O_2 was more than 10 μmol/l, the calibration curve was turned to level off, which was the typical characteristic of the Michaelis–Menten kinetic mechanism. The apparent Michaelis–Menten constant (K_m^{app}) can be calculated from the electrochemical version of the Lineweaver–Burk equation [38]:

$$\frac{1}{I_{ss}} = \frac{1}{I_{max}} + \frac{K_M^{app}}{I_{max}c}$$

where I_{ss} is the steady current after the addition of substrate, c is the bulk concentration of the substrate, and I_{max} is the maximum current measured under saturated substrate condition. The K_m^{app} value was determined by analysis of the slope and the intercept of the plot of the reciprocals of the reduction peak current vs H_2O_2 concentration, which was an indicative of the enzyme–substrate kinetics. The small value of K_m^{app} means higher enzymatic activity of immobilized enzyme. Based on this equation, the K_m^{app} value was calculated as 9.86 μmol/l.

The SA/nano-SiO_2/$BMIMPF_6$/Hb/CPE is also sensitive to the presence of O_2. With the injection of different amounts of air into an aerobic pH 7.0 PBS by a syringe, the cyclic voltammograms were recorded and shown in Fig. 5. It can be seen that a significant increase of the reduction peak current at about −0.448 V appeared and accompanied by the decrease of the oxidation peak current. The more air injected, the higher the reduction peak appeared (curve c–i).

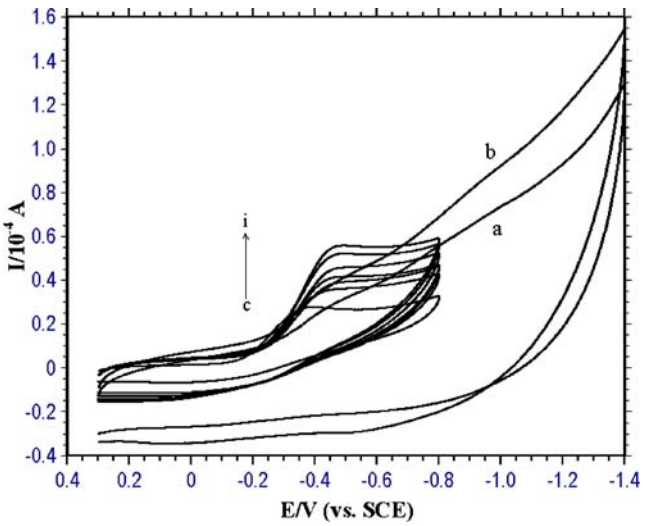

Fig. 5 Cyclic voltammograms of SA/nano-SiO_2/$BMIMPF_6$/CPE in 5 ml of 0.1 mol/l pH 7.0 PBS containing **a** 0 and **b** 10 ml air, and SA/nano-SiO_2/$BMIMPF_6$/Hb/CPE in 5 ml of 0.1 mol/l pH 7.0 PBS containing 0, 2, 10, 13, 25, 30, 35 ml air (curve *c–i*), respectively, with the scan rate as 100 mV/s

The results indicated that the formed heme Fe(II) had reacted with oxygen dissolved in the solution. The catalytical efficiency, which was expressed as the ratio of the reduction peak current of heme Fe(III) in the presence of (I_c) and the absence of oxygen (I_d), decreased with the increase of scan rate. The concentration of O_2 dissolved in the solution can be calculated from the dissolution of air. The result was the characteristics of electrochemical catalytic reduction of oxygen. The catalytical reduction of O_2 can be elucidated with the following procedure [39]:

$$\text{Hb Fe(III)} + \text{e} + \text{K}^+_{(\text{aq})} \rightarrow \text{Hb Fe(II)} + \text{K}^+_{(\text{film})}$$

$$\text{Hb Fe(II)} + \text{O}_2 \rightarrow \text{Hb Fe(II)..O}_2$$

$$\text{Hb Fe(II)..O}_2 + \text{K}^+_{(\text{film})} + 2\text{H}_2\text{O} + 2\text{e}^- \rightarrow \text{Hb Fe(II)} + \text{H}_2\text{O}_2 + 2\text{OH}^- + \text{K}^+_{(\text{aq})}$$

where Hb Fe(III) and Hb Fe(II) indicate met Hb and ferrous Hb, respectively, and Hb Fe(II)..O_2 denotes the oxygenated ferrous Hb.

The stability of this SA/nano-SiO_2/$BMIMPF_6$/Hb/CPE electrode had been examined as well. After being exposed to air and placed in the refrigerator for 15 days, the cyclic voltammetric peak currents decreased about 4.0%.

Electrochemical impedance spectroscopy

The typical Nyquist plot includes a semicircle portion at higher frequency corresponding to the electron-transfer limited process and a linear part at lower frequency indicating that an ion diffusion-limited process plays the major role and there is no ion insertion reaction at the electrode/RTILs interface. Therefore, electrochemical impedance spectroscopy (EIS) is a valuable method to give information on the impedance changes of the modified electrode, and the semicircle diameter of EIS equals the electron transfer resistance (R_{ct}). The value of R_{ct} varies when different substances are adsorbed on the electrode surface. By using 5.0×10^{-3} mol/l $Fe(CN)_6^{3-/14-}$ solution as redox probe, the EIS of different modified electrode were recorded, and the results were shown in Fig. 6. Curve a showed the EIS of the bare CPE, which had a big semicircle domain and indicated a big electron transfer resistance (R_{ct}=1,538 Ω). The result was due to the nonconductive paraffin that existed in the carbon paste. Curve c was the SA/nano-SiO_2/$BMIMPF_6$-film-modified CPE; the R_{ct} value was 509 Ω, indicating that the presence of SA/nano-SiO_2/$BMIMPF_6$ film can facilitate the electron transfer. IL has high ionic conductivity, and nano-SiO_2 is an inorganic nonmetallic material, which can give the protein molecules more freedom in orientation and provide an environment similar to the native environment

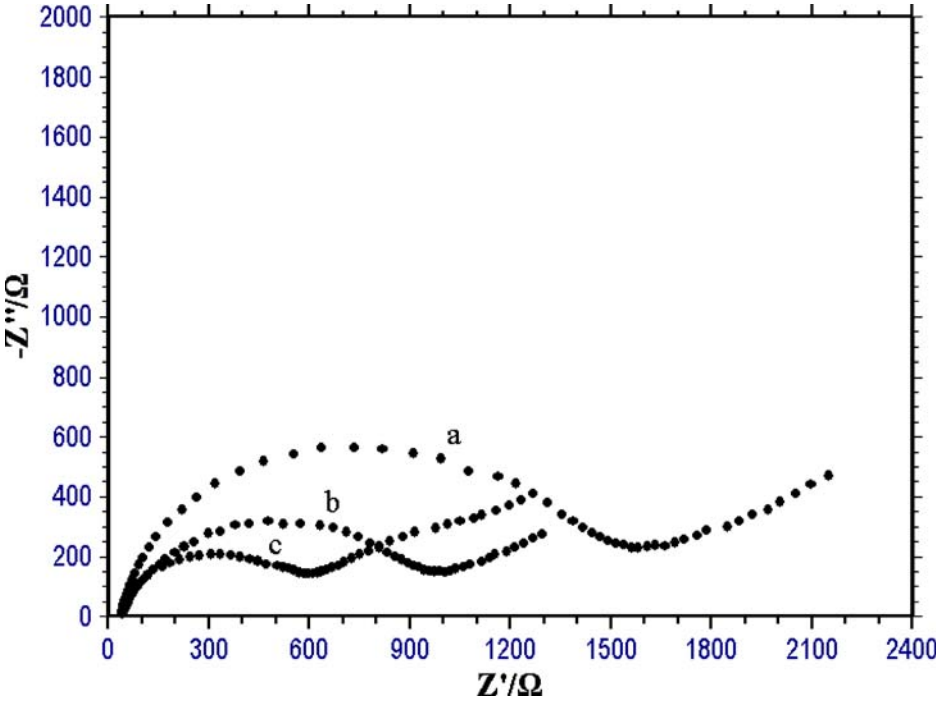

Fig. 6 Electrochemical impedance spectroscopy (EIS) of **a** CPE, **b** SA/nano-SiO_2/$BMIMPF_6$/Hb/CPE, and **c** SA/nano-SiO_2/$BMIMPF_6$/CPE, with the frequencies range from 10^4 to 0.5 Hz and a 5.0×10^{-3} mol/l $Fe(CN)_6^{3-/4-}$ solution containing 0.1 mmol/l KCl

for electron transfer of redox protein [40]. Therefore, the presence of IL and nano-SiO_2 can enhance the electron transfer process. However, on SA/nano-SiO_2/$BMIMPF_6$/Hb-film-modified electrode, the R_{ct} got was 991 Ω (curve b). The presence of Hb in the composite film obstructed the electron transfer, and the R_{ct} was higher than that of SA/nano-SiO_2/$BMIMPF_6$ film. The difference of R_{ct} value indicated the different interface status of film.

Cyclic voltammetric results of $Fe(CN)_6^{3-14-}$ solution is also a valuable and convenient method to monitor the barrier of the modified electrode. Figure 7 showed cyclic voltammograms of different modified electrodes. A pair of well-defined redox peaks was observed at the bare CPE (curve b). When SA/nano-SiO_2/$BMIMPF_6$/Hb was cast on the electrode, the cyclic voltammetric curve decreased

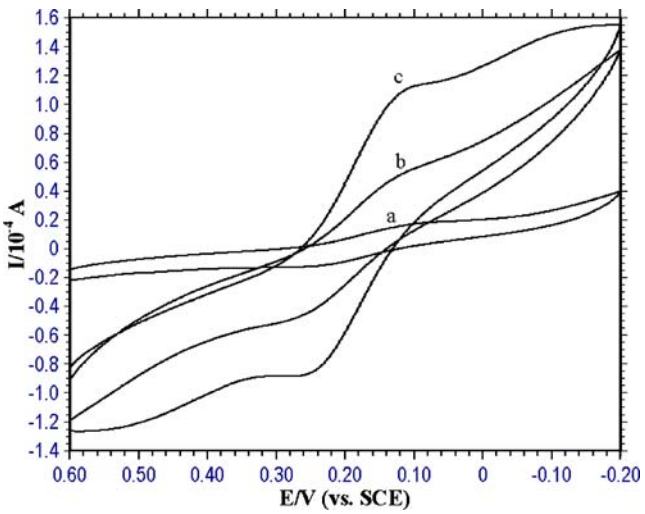

Fig. 7 Cyclic voltammograms of **a** SA/nano-SiO_2/$BMIMPF_6$/Hb/CPE, **b** CPE, and **c** SA/nano-SiO_2/$BMIMPF_6$/CPE in a 5.0×10^{-3} mol/l $Fe(CN)_6^{3-14-}$ solution containing 0.1 mmol/l KCl with the scan rate as 100 mV/s

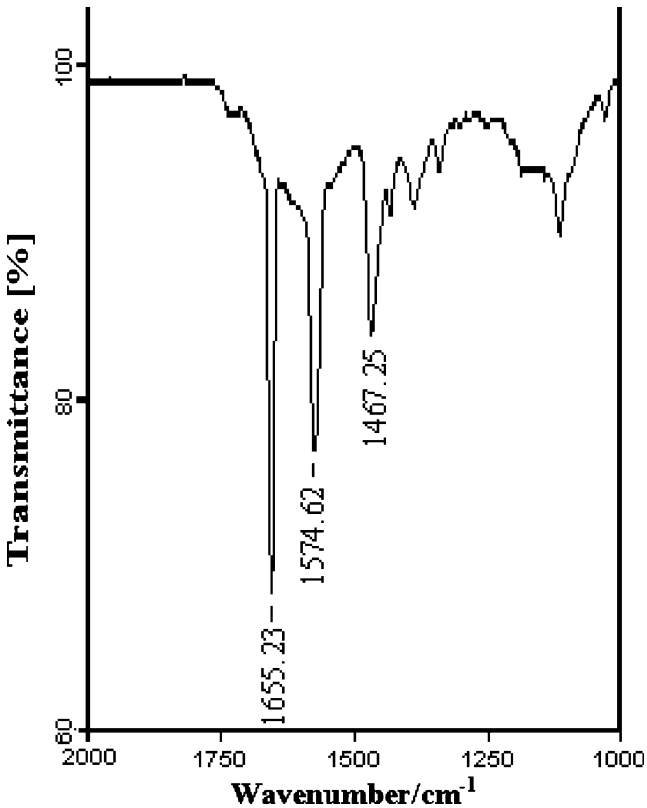

Fig. 8 FT-IR spectra of Hb in SA/nano-SiO_2/$BMIMPF_6$ film

drastically (curve a), implying that Hb blocked the diffusion of $Fe(CN)_6^{3-14-}$ to the surface of electrode. While on SA/nano-SiO_2/$BMIMPF_6$/CPE, the electrochemical response of $Fe(CN)_6^{3-14-}$ was increased greatly (curve c), which also indicated that the presence of $BMIMPF_6$ and nano-SiO_2 can promote the electron transfer procedure.

FT-IR measurement of conformational change

Fourier transform infrared (FT-IR) spectroscopic technique has been employed to study the conformational change of Hb. FT-IR is very sensitive to the conformational changes of the protein, which will affect the electron transfer reactivity. It has been known that the shapes of amide I and amide II infrared absorption band of Hb can provide detailed information about the secondary structure of the polypeptide chain. The amide I band (1,700~1,600 cm^{-1}) is caused by C=O stretching vibrations of peptide linkages in the protein's backbone, and the amide II band (1620~1500 cm^{-1}) is attributed to the combination of N–H bending and C–N stretching [41]. Figure 8 showed the FT-IR spectra of Hb in the SA/nano-SiO_2/$BMIMPF_6$/Hb composite film. It can be seen that the absorption bands of Hb are located at 1,655.23 and 1,574.62 cm^{-1}, which reflect the situation of α helix and anti-β sheet in the protein, respectively. The results was nearly the same as those of the native Hb conformation [36], which proved that Hb in the bionanocomposite film was not denatured and retained its native structure.

Conclusion

In this paper, a new kind of bionanocomposite matrix for the immobilization of Hb was fabricated by mixing SA, nano-SiO_2, and $BMIMPF_6$ together. Hb retained its bioactivity in the composite film, and the direct electrochemistry of Hb in the SA/nano-SiO_2/$BMIMPF_6$ film was carefully investigated. The Hb-film-modified CPE showed good enhanced electrocatalytic activity to the reduction of TCA, hydrogen peroxide (H_2O_2), and oxygen (O_2). The direct electron transfer of Hb with the electrode surface may be attributed to cooperate with the biocompatibility of SA, unique properties of nano-SiO_2, and higher ionic conductivity of $BMIMPF_6$. The SA/nano-SiO_2/$BMIMPF_6$/Hb/CPE showed higher stability and was a potential third-generation biosensor.

Acknowledgments We are grateful to the financial support of the National Natural Science Foundation of China (No. 20405008, 20635020) and the Open Foundation of State Key Laboratory of Chemo/Biosensing and Chemometrics of Hunan University (200615).

References

1. Nakashima N, Ando R, Kunitaka T (1983) Chem Lett 11:1577
2. Nassar AEF, Willis WS, Rusling JF (1995) Anal Chem 67:2386
3. Ray A, Feng ML, Tachikawa H (2005) Langmuir 21:7456
4. Lu HY, Yang J, Rusling JF, Hu NF (2006) Electroanalysis 18:379
5. Yang J, Hu NF (1999) Bioelectrochem Bioenerg 48:117
6. Chen X, Peng X, Kong J (2000) J Electroanal Chem 480:26
7. Pang JT, Fan CH, Liu XJ, Chen T, Li GX (2003) Biosens Bioelectron 19:441
8. Fan CH, Wang HY, Sun S, Zhu DX, Wagner G, Li GX (2001) Anal Chem 73:2850
9. Rusling JF (1998) Acc Chem Res 31:363
10. Rhoten MC, Hawkridge FM, Wilezek J (2002) J Electroanal Chem 535:97
11. Wang J, Li M, Shi Z, Li N, Gu Z (2002) Anal Chem 74:1993
12. Luo XL, Killard AJ, Smyth MR (2006) Electroanalysis 18:1131
13. Buzzeo MC, Hardace C, Compton RG (2004) Anal Chem 76:4583
14. Hiroyuki O (2005) Electrochemical aspects of ionic liquids. Wiley, New York
15. Liu JF, Jonsson JA, Jiang GB (2005) Trend Anal Chem 24(1):20
16. Compton DL, Laszlo JA (2002) J Electroanal Chem 520:71
17. Endres F (2004) Zeitschrift fur Physikalische Chemie 218:255
18. Rozniecka E, Shul G, Sirieix-Plenet J, Gaillon L, Opallo M (2005) Electrochem Commun 7:299
19. Rozniecka E, Niedzidka J, Sirieix–Plenet J, Gaillon L, Murphy MA, Marken F, Opallo M (2006) J Electroanal Chem 587:133
20. Shul G, Sirieix–Plent J, Gaillon L, Opallo M (2006) Electrochem Commun 8:1111
21. Lu XB, Hu JQ, Yao X, Wang ZP, Li JH (2006) Biomacromolecules 7:975
22. Lu XB, Zhang Q, Zhang L, Li JH (2006) Electrochem Commun 8:874
23. Zhang YJ, Shen YF, Li JH, Li N, Dong SJ, Ivaska A (2005) Langmuir 21:4797
24. Zhao F, Wu X, Wang M, Liu Y, Gao L, Dong SJ (2004) Anal Chem 76:4960
25. Sun W, Wang DD, Gao RF, Jiao K (2007) Electrochem Commun 9:1159
26. Sun H (2006) J Porous Mater 13:393
27. Li Y, Shi XW, Hao JC (2006) Carbon 44:2664
28. Liu Y, Wang MJ, Li J, Li ZY, He P, Liu HT, Li JH (2005) Chem Commun 1778
29. Maleki N, Safavi A, Tajabadi F (2006) Anal Chem 78:3820
30. Sun W, Gao RF, Bi RF, Jiao K (2007) Chinese J Anal Chem 35:567
31. Yan QP, Zhao FQ, Li GZ, Zeng BZ (2006) Electroanalysis 18:1075
32. Zhao YF, Gao YQ, Zhan DP, Liu H, Zhao Q, Kou Y, Shao YH, Li MX, Zhuang QK, Zhu ZW (2005) Talanta 66:51
33. Li CM, Zang JM, Zhan DP, Chen W, Sun CQ, Teo AiL, Chua YT, Lee VS, Moochhala SM (2006) Electroanalysis 18:713
34. Sun W, Yang MX, Gao RF, Jiao K (2007) Electroanalysis 19:1597
35. Luo XL, Xu JJ, Zhao W, Chen HY (2004) Sensor Actuat B Chem 97:249
36. Wang SF, Chen T,Zhang ZL, Shen XC, Lu ZX, Pang DW, Wong KY (2005) Langmuir 21:9260
37. Fan CH, Zhuang Y, Li GX, Zhu JQ, Zhu DX (2000) Electroanalysis 12:1156
38. Kamin RA, Willson GS (1980) Anal Chem 52:1198
39. Fan CH, Liu XJ, Pang JT, Li GX, Scheer H (2004) Anal Chim Acta 523:225
40. Tian Y, Shioda M, Kasahara S, Okajima T, Mao L, Hisabori T, Ohsaka T (2002) Biochim Biophys Acta 1569:151
41. Kauppien JK, Moffatt DJ, Mantsch HH, Cameron DG (1981) Appl Spectrosc 35:271